Chilean J. Agric. Anim. Sci., ex Agro-Ciencia (2024) 40(1): 44-55.
https://doi.org/10.29393/CHJAAS40-5CDER40005

ISSN 0719-3890 online

CONVECTIVE DRYING KINETICS OF YACON (*Smallanthus sonchifolius* Poepp. & Endl.) SLABS AND EVALUATION OF THE DRYER PID TEMPERATURE CONTROL SYSTEM

Edwin O. Baldeón [1a,2*], Walter F. Salas-Valerio [1b,2], Julio M. Vidaurre-Ruiz [1c,2], and Raúl Comettant-Rabanal [3]

[1a] Departamento de Ingeniería de Alimentos y Productos Agropecuarios, Facultad de Industrias Alimentarias, Universidad Nacional Agraria La Molina, Lima, Peru
https://orcid.org/0000-0003-0229-8317
[1b] Departamento de Ingeniería de Alimentos y Productos Agropecuarios, Facultad de Industrias Alimentarias, Universidad Nacional Agraria La Molina, Lima, Peru
https://orcid.org/0000-0002-4143-4003
[1c] Departamento de Ingeniería de Alimentos y Productos Agropecuarios, Facultad de Industrias Alimentarias, Universidad Nacional Agraria La Molina, Lima, Peru
https://orcid.org/0000-0003-0980-9474
[2] Grupo de Investigación en Ingeniería de Alimentos, Universidad Nacional Agraria La Molina, Lima, Peru
[3] Escuela Profesional de Ingeniería Agroindustrial, Facultad de Ingenierías, Universidad Privada San Juan Bautista. Carretera Panamericana Sur Ex km 300, La angostura – Subtanjalla, CP 11004. Ica, Peru
https://orcid.org/0000-0001-5485-1271
* Corresponding author: eobch@lamolina.edu.pe

ABSTRACT

Yacon is a functional food that is rich in fructooligosaccharides (FOS) and highly perishable, which requires inexpensive methods for its preservation. The objectives of this research were to model the kinetics of convection drying of yacon slabs and to assess the effect of air velocity on the temperature record of the heating zone controlled by the Proportional-Integral-Derivative control system (PID). Different temperatures (60, 70, and 80 °C) at constant air velocity (0.87 m s^{-1}) were evaluated in a convective tray drying system. To determine the effect of air velocity on the PID temperature controller, different air velocities (0.81-2.06 m s^{-1}) at constant temperature (70 °C) were studied. The results showed that Page's model was the best fitting of the data obtained, the effective diffusivity of convective drying of yacon ranged from $1.22x10^{-10}$ to $1.9x10^{-10}$ m^2 s^{-1} and the activation energy was 21.76 kJ mol^{-1}. With PID temperature control, it was observed that the best drying rate and lowest temperature signal error occurred at an air velocity of 1.46 m s^{-1}, where the temperature signal was more stable and closer to the reference temperature. In conclusion, the kinetic modeling of the convective drying of yacon provides optimal drying parameters as well as behavior of mass and heat transfer phenomena, particularly considering that the effect of air velocity influences the drying kinetics and the PID temperature control of the dryer.

Keywords: Page model, effective diffusivity, activation energy, hot air drying, Fick's second law.

Received: November 7, 2023 Accepted: April 1, 2024

INTRODUCTION

Yacon (*Smallanthus sonchifolius* Poepp. and Endl.) is a root crop indigenous to the Andean region and has been widely cultivated globally, including countries such as Brazil, the Czech Republic, Ecuador, Germany, Japan, and New Zealand (Khajehei et al., 2018). It is considered a functional food, low in calories, slightly sweet, and rich in biologically active components with a low degree of polymerization, such as inulin and β-(2→1) fructooligosaccharides (FOS), both considered prebiotics that provide multiple benefits to human health. In addition, their contribution in dietary fiber contributes to lowering blood glucose levels in diabetic patients (Mejía-Águila et al., 2021; Oliveira et al., 2013). However, the high water content of yacon makes it highly perishable, requiring inexpensive processing techniques to obtain a quality and commercially stable product.

In this sense, convective drying is a low-cost water removal process using hot airflow, where heat, mass, and movement quantity transfer phenomena occur simultaneously (Castro et al., 2018). The main mechanisms driving internal and external mass transport are diffusion, convection, and evaporation. In mathematically modeling drying processes, the conduction of heat can be expressed using Fourier's law, a widely recognized principle (Khan et al., 2022). Under this process, food stability is improved, since mobility and water activity (a_w) are greatly reduced and, consequently, physical, chemical, enzymatic, and microbiological changes during storage are minimized, thereby extending the shelf-life of the food (Amit et al., 2017; Franco et al., 2017).

Drying kinetics describes the moisture change over time during food drying. It is of great importance to determine the drying curve, which is affected by several factors. External factors include temperature, velocity, and relative humidity of air. On the other hand, internal factors include moisture content, composition, texture, porosity, as well as macro- and microstructure of food (Castro et al., 2018). Drying kinetics modeling is a mathematical tool to understand the water migration behavior of a food matrix, helping optimize and establish better criteria for dryer design. For this purpose, there are theoretical methods adjusted to drying mechanisms by molecular diffusion based on Fick's second law.

Empirical methods attempt to describe the drying process experimentally but lack a complete understanding of its overall behavior. While semi-empirical methods adjust and explain the drying mechanisms associated with capillarity and condensation, based on Newton's Law, including the models of Lewis, Henderson and Pabis, Page, and others (Inyang et al., 2018; Sahoo et al., 2022). In particular, in food drying, mathematical models are applied to describe the behavior of the drying kinetics. This implies using mass and heat transfer from inside the food, in some cases by diffusion and in other cases by external resistance to the food surface (Inyang et al., 2018; Sahoo et al., 2022).

For this reason, previous studies by Bernstein and Noreña (2014); Marques et al. (2023); Marques et al. (2022a); and Marques et al. (2022b) have studied the parameters, kinetics, and modeling of the yacon drying process. Campos et al. (2016) determined the drying temperature (80 °C) for rapid dehydration without affecting the FOS content; and Gangta et al. (2023) studied the pre-drying treatment to avoid browning of yacon powder. However, there are no reports on the influence of high air velocity on heat transfer and its effect on Proportional-integral-derivative (PID) systems for effective and genuine drying temperature control, which are useful for maintaining the organoleptic and nutraceutical quality of yacon. Therefore, temperature control is of utmost importance in industrial processes, especially in food processing during heating and cooling (e.g., baking, freezing, drying, and others). PID control is the most popular in process applications, due to its simplicity, stability, and low cost (Dubey et al., 2022). However, it has some limitations associated with parameter tuning, timing systems, etc. (Álvarez de Miguel et al., 2017; Sungthong and Assawinchaichote, 2016).

As mentioned above, temperature and air velocity are factors affecting water removal rate during food drying (Boeri et al., 2013). Therefore, the control of these factors is very important in drying, as the desired moisture content of the food will be achieved if the temperature and air velocity are appropriate. Meanwhile, Sungthong and Assawinchaichote (2016) investigated the ability to control temperature in response to air velocity variation in an electrically heated dryer. Therefore, the goals of this research were to model the kinetics of convective drying of yacon slabs and to evaluate the effect of air velocity on PID control.

MATERIALS AND METHODS

Samples

The yacon samples were obtained from a local market (La Molina, Lima, Peru) and stored refrigerated at approximately 8 °C. The moisture content of fresh yacon samples was determined

using the method 930.04 (AOAC, 2005). Furthermore, the moisture content of the samples was 87.18 ± 0.56%, which is consistent with the values documented in previous studies (Cuervo et al., 2018; Salinas et al., 2018).

Preparation of yacon samples

The yacon samples were washed with plenty of water, sliced using a vegetable slicer (CL-52, Robot Coupe, United States) into 5-mm-thick slices, and then immersed in a 0.2% citric acid solution for 20 min to prevent enzymatic browning (Marques et al., 2022a). Subsequently, they were cut with a knife into 1 x 1 x 0.5 cm slabs (length x width x thickness).

Drying procedure

The yacon samples were submitted to drying using a hot air tray dryer (Edibon model SBANC, Spain). Then the samples were evenly distributed over three 3-mm mesh trays, with each tray covering a drying area of 10 x 10 cm. The average load of yacon in the dryer was 230 g. The drying temperatures were 60, 70, and 80 °C and the air velocity was 0.87 m s^{-1}. Under the weight control system of the dryer, weight was recorded automatically every second until a consistent weight was achieved, resulting in thousands of weight data. The data were then compressed using Excel, with the weight being recorded every 15 min during the first hour of drying and every 30 min thereafter until the end of drying. Three drying repetitions were carried out for each temperature.

Yacon drying curves

The drying curves were constructed by plotting free moisture content data against time, and the drying rate curve was plotted against free moisture content. These curves were also used to determine drying rate periods and drying time. The free moisture content (X) was calculated from the moisture content and the equilibrium moisture content (Xe), expressed in kg of water per kg of dry matter, according to Eq. 1.

$$X = X' - Xe' \quad (1)$$

Where Xe′ was experimentally obtained after the material was subjected to a long period of drying, reaching a constant moisture content (Corrêa et al., 2021; Oliveira et al., 2021). The drying rate was calculated as the kilograms of water removed per kilogram of dry matter per hour, as shown in Eq. 2.

$$\text{Drying rate} = \Phi = -\frac{dX}{dt} = \frac{\Delta X}{\Delta t} \quad (2)$$

Where Φ is the drying rate ($kg_w\ kg_{dm}^{-1}\ h^{-1}$), X is the free moisture ($kg_w\ kg_{dm}^{-1}$) and t is the time of drying (h).

Drying kinetics modeling

The drying kinetics was determined from the falling rate drying period as the moisture ratio (MR) vs drying time, according to Eq. 3.

$$MR = \frac{X' - X_e'}{X_c' - X_e'} = \frac{X}{X_c} \quad (3)$$

Where X′, Xc′, and Xe′ are moisture contents at any time, critical moisture content, and equilibrium moisture content ($kg_w\ kg_{dm}^{-1}$), respectively. Therefore, X and Xc are free moisture content at any time, and free critical moisture content ($kg_w\ kg_{dm}^{-1}$), respectively. Mathematical models were selected due to their extensive use in indicating the drying behavior of food matrices. Table 1 shows the mathematical models to model the drying kinetics of yacon.

Determination of effective moisture diffusivity and activation energy

Fick's second law of diffusion in an unsteady state was used to describe the mass transport during the yacon slabs (Compaoré et al., 2019;

Table 1. Mathematical models to describe yacon slabs.

Model Name	Model Equation	Reference
Fick	$MR = \frac{8}{\pi^2} e^{-kt}$	Corrêa et al. (2021)
Newton	$MR = e^{-kt}$	Royen et al. (2020)
Henderson y Pabis	$MR = ae^{-kt}$	Royen et al. (2020) Lisboa et al. (2018)
Page	$MR = e^{-Kt^n}$	Royen et al. (2020) Lisboa et al. (2018)

Cruz et al., 2015; Khwaja et al., 2020; Sahoo et al., 2022), as followed Eq. 4.

$$\frac{\partial X}{\partial t} = D_{eff}\frac{\partial^2 X}{\partial r^2} \quad (4)$$

Where X is the water content ($kg_w\ kg_{dm}^{-1}$), t is time (s), D_{eff} is the effective moisture diffusivity ($m^2\ s^{-1}$), and r is the spatial coordinate, varying from 0 to L, with L the half-thickness (m). Based on certain assumptions, such as uniform sample moisture distribution, central symmetric mass transfer, negligible shrinkage during drying, and constant diffusion coefficient (Compaoré et al., 2019; Cruz et al., 2015), Compaoré et al., 2019), the initial and boundary conditions of Eq. (4) are:

$$For\ f(x) = \begin{cases} X = Xo,\ t = 0 \\ \partial X/\partial r,\ r = 0 \\ X = Xe,\ r = L \end{cases} \quad (4)$$

Analytical solution of Eq. (4) can be solved in terms of an infinite series of slabs (Compaoré et al., 2019; Khwaja et al., 2020; Oliveira et al., 2021), according to Eq. (5).

$$MR = \frac{8}{\pi^2}\sum_{n=0}^{\infty}\frac{1}{(2n+1)^2}exp\left(\frac{(2n+1)^2\pi^2 D_{eff}t}{4L^2}\right) \quad (5)$$

Where n is the number of terms in the series. If the drying time is long, a simplified equation can be simplified to the first term without loss of accuracy (Cruz et al., 2015; Sahoo et al., 2022), as shown in Eq. (6).

$$MR = \frac{8}{\pi^2}exp\left(\frac{-\pi^2 D_{eff}}{4L^2}t\right) \quad (6)$$

The above equation is further simplified by taking the logarithm of both sides (Compaoré et al., 2019; Cruz et al., 2015; Khwaja et al., 2020; Sahoo et al., 2022), as shown in Eq. (7).

$$\ln(MR) = ln\left(\frac{8}{\pi^2}\right) - \frac{\pi^2 D_{eff}}{4L^2}t \quad (7)$$

The slope can be calculated by plotting the regression graph ln (MR) versus drying time. Eq. (8) can be used to estimate the effective moisture diffusion (D_{eff}).

$$slope = \frac{\pi^2 D_{eff}}{4L^2} \quad (8)$$

The temperature-dependency of effective diffusivity can be explained with the Arrhenius equation (Compaoré et al., 2019; Cruz et al., 2015; Khwaja et al., 2020; Oliveira et al., 2021; Sahoo et al., 2022), as presented by Eq. (9).

$$D_{eff} = D_0 exp\left(\frac{E_a}{RT}\right) \quad (9)$$

Where D_0 is the pre-exponential factor of the Arrhenius equation ($m^2\ s^{-1}$), E_a is the activation energy ($kJ\ mol^{-1}$), R is the universal gas constant (8.314 $J\ mol^{-1}K^{-1}$), and T is the drying air temperature (K).

The activation energy was determined by plotting ln (D_{eff}) versus (1/T). This produced a straight line with an intercept equal to ln (D_0) and slope equal to ($E_a\ R^{-1}$), enabling the estimation of values for both D_0 and E_a (Cruz et al., 2015; Khwaja et al., 2020; Oliveira et al., 2021), as shown in Eq. (10).

$$\ln D_{eff} = \ln D_0 - \frac{E_a}{R}\frac{1}{T} \quad (10)$$

Analysis of PID temperature control system

The yacon samples were dried in a computer-controlled tray dryer (Fig. 1a). The parts of this dryer were described by Gamboa-Santos et al. (2013). It has four sections: 1) fan (air velocity control), 2) 2000 W electric heater, 3) temperature control system, and 3) drying chamber (load cell and trays). The airflow was parallel to the sample and the drying air velocity was measured with an anemometer (840003, Sper Scientific, Taiwan) inside the drying chamber.

The yacon samples were dried at 70 °C recommended by Lisboa et al. (2018) at different air velocities from 0.81, 1.2, 1.46, 1.67, 1.89, and 2.06 m s^{-1}. Additionally, the dryer has a PID control system (Fig. 1b) and the reference temperature (Tr) was set at 70 °C. In addition, temperature measurements were recorded: air temperature after heating (TS3) and air temperature entering the drying chamber (TS4). The distance between the heating zone and the drying zone is 38 cm. The PID controller is used to control the temperature inside the dryer. In this sense, the gains of the PID control are adjusted to correct the error (e) between Tr and TS. Thus, e(t) is expressed in Eq. (11).

$$e(t) = Tr(t) - TS(t) \quad (11)$$

The stability comparison of the signals of TS(t) for any time and different air velocities was determined by the standard error (), and by the integral absolute error (IAE) criterion as proposed in the literature (Gani et al., 2019; Mahmood et al., 2018; Wu et al., 2019; Mahmood et al., 2018). Next, equation 12 represents the standard error ($\sigma_{\bar{x}}$).

$$\sigma_{\bar{x}} = \frac{\sigma}{\sqrt{n}} \ldots (12)$$

Where σ is the standard deviation and n is the sample size. Equation 13 expresses the integral absolute error (IAE).

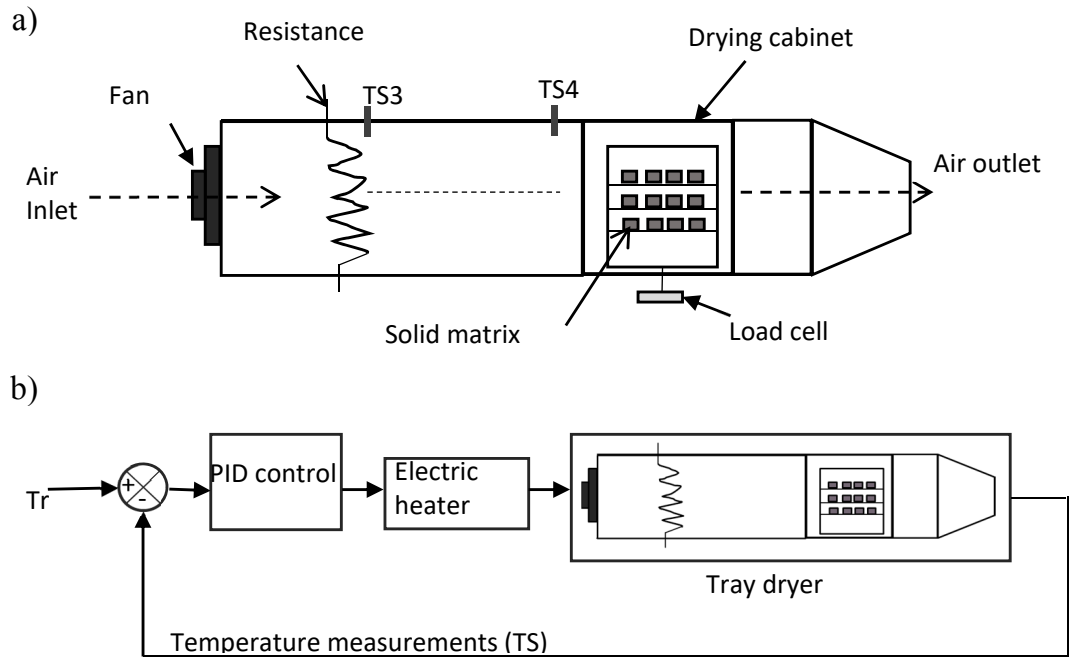

Fig. 1. Parts of the dryer (a) and PID temperature control system (b) in the convective drying of yacon slabs.

$$\text{IAE} = \int_0^{\infty} |e(t)| dt \qquad (13)$$

Statistical design and analysis

A Completely Randomized Design (CRD) was used to analyze the data of times, critical humidity, critical velocity, and effective diffusivity. An analysis of variance (ANOVA9 and the LSD mean comparison test (95 % confidence level) were also used. All the statistical analyses were conducted using the statistical package Statgraphics Centurion 19 (StatPoint, Inc., USA). Additionally, the drying kinetics data were fitted by non-linear regression using the Solver tool of Excel 2019 (Microsoft, USA). Finally, the fit between experimental and calculated values was evaluated using the coefficient of determination (R^2) and the root mean square error (RMSE).

$$RMSE = \left[\frac{1}{N}\sum_{N}^{I=1}\left(MR_{Mod} - MR_{Exp}\right)^2\right]^{1/2} \qquad (14)$$

Where MR_{Mod} is the moisture ratio determined by the model and MR_{Exp} is the moisture ratio calculated from the experimental data.

RESULTS AND DISCUSSION

Drying curves of yacon

The effect of drying temperature on the convective drying characteristics of yacon slabs is plotted in Fig. 2. As shown in Fig. 2a, the free moisture content decreases with drying time due to the removal of water during convective drying until equilibrium moisture is reached. Additionally, the decrease in time is accentuated by the increase in drying temperature from 50 to 70 °C. In food drying, a higher rate of heat and mass transfer is obtained as temperature increases because there is greater movement of water molecules inside the material. Furthermore, this can be attributed to the increase in vapor pressure and diffusivity (Botelho et al., 2011; Corrêa et al., 2021; Sahoo et al., 2022; Salinas et al., 2018).

Fig. 2b shows the existence of two periods of drying rate: (i) a first period of constant drying rate at the beginning of drying, when water from the yacon surface is eliminated by evaporation; (ii) a second period after the critical point, when decreasing drying rate triggers the water inside the yacon is transferred by molecular diffusion. Similarly, Marques et al. (2023) conducted a study on drying yacon using an experimental drying device that enabled continuous recording of mass, sample volume, and exchange surface area. Their findings indicated two periods of yacon drying, with the drying curve being corrected for the actual exchange surface area of the sample. Likewise, Botelho et al. (2011) observed two periods of drying rate for carrots.

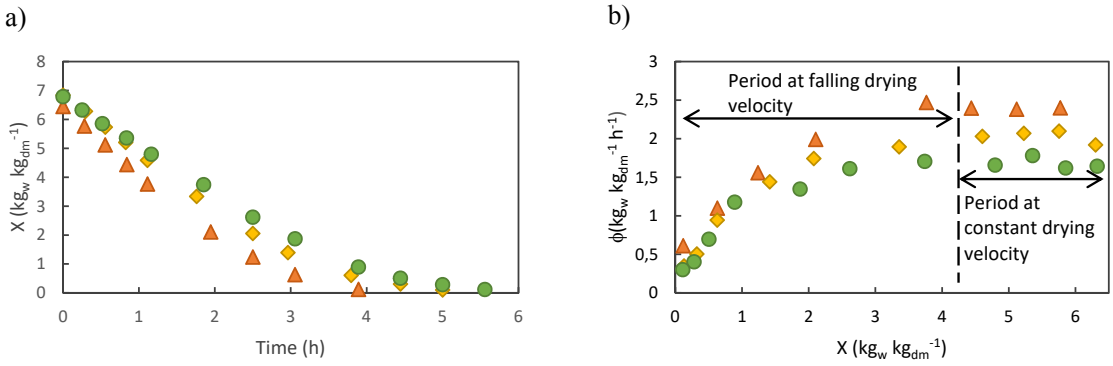

Fig. 2. The curves (a) and velocity (b) of convective drying of drying yacon slabs at different drying temperatures: 60 °C (●), 70 °C (♦), and 80 °C (▲)

Modeling of drying kinetics

Table 2 shows the parameters, constants, and statistics of the models. As a result, the constant k increased with increasing temperature for all the models.

Mass transfer was improved during convective drying of yacon slabs. Similar results were reported by Lisboa et al. (2018) in the convective drying of yacon cylinders and Sahoo et al. (2022) in the convective drying of yam slices. Accordingly, the model that best describes the drying behavior for all temperatures was the Page model since the value of R-squared was higher and the value of RMSE was lower. The model also proved the most efficient in previous studies conducted by Lisboa et al. (2018) in the convective drying of yacon cylinders; Oliveira et al. (2021) in the pulsed vacuum osmotic dehydration of yacon; Simal et al. (2005) in the convective drying of kiwi fruit; and Razola-Díaz et al. (2023) in the convective drying of orange by-products.

Effective moisture diffusivity and activation energy

Table 3 shows the effective moisture diffusivity values (D_{eff}) in the convective drying of yacon slabs. As a result, D_{eff} values from $1.22x10^{-10}$ to $1.90x10^{-10}$ m^2 s^{-1} ranged between 60 to 80 °C. In the drying of yacon cylinders, Lisboa et al. (2018) obtained D_{eff} values from $1.18x10^{-9}$ to $2.15x10^{-9}$ m^2 s^{-1} for temperature ranges from 50 to 70 °C. Likewise, Botelho et al. (2011) conducted a study in the drying of carrot slices and found D_{eff} values from $8.94x10^{-10}$ to $3.57x10^{-9}$ m^2 s^{-1} for temperature ranges from 50 °C to 100 °C. In the convective drying of yam slices, moisture diffusivity ranged from $4.51x10^{-10}$ to $7.52x10^{-10}$ m^2 s^{-1}, while moisture diffusivity values for food are between 10^{-11} and 10^{-9} m^2 s^{-1} (Sahoo et al.,2022).

In the convective drying of yacon slabs, an increase in D_{eff} was found with increasing temperature. As a consequence, water movement increases with temperature from inside the pores, thus overcoming the internal resistance of mass transfer, and with it the increase in water diffusivity (Botelho et al., 2011; Corrêa et al., 2021; Lisboa et al., 2018). In addition, it can be associated with various factors such as sample variety, sample size, pre-treatment, and type of dryer (Sahoo et al., 2022; Shi et al., 2013).

Activation energy (E_a) is described as the energy required to initiate the release of moisture from the inside to the outside of the food. If the E_a is higher and the water is strongly bound, then the release of moisture will be slower (Keneni et al., 2019; Sahoo et al., 2022). Next, the E_a in the convective drying of yacon slabs was 21.76 kJ mol^{-1} and the pre-exponential factor (D_0) was $3.14x10^{-7}$ m^2 s^{-1}. Likewise, Corrêa et al. (2021) in the vacuum osmotic dehydration of yacon, the activation energies obtained were 28.66 and 20.07 kJ mol^{-1}. Additionally, Sahoo et al. (2022) reported that the E_a was 23.53 kJ mol^{-1}in the convective drying of yam slices.

Analysis of PID temperature control system

In Fig. 3, the impact of air velocity on the convection drying curve of yacon slabs is demonstrated. The findings indicate that as the air velocity rises from 0.81 to 1.46 m s^{-1}, the drying time decreases, particularly at an air velocity of 1.46 m s^{-1}. However, there is no notable difference in drying time when the air velocity is increased from 1.67 to 2.06 m s^{-1}. This implies that a specific air velocity facilitates enhanced water elimination.

When air velocities are higher, there is an increase in moisture removal. However, this also leads to a hardening of the material (Zheng et al., 2023). During the falling rate period of drying,

Table 2. Parameters, constants, and statistics of the models convective drying kinetics of yacon slabs.

Temperature (°C)	Model	n	a	k	R^2	RMSE
60	Fick	-	0.8106	0.4526	0.991	0.116
	Newton	-	-	0.5484	0.982	0.059
	Henderson and Pabis	-	1.0588	0.5775	0.978	0.054
	Page	1.4418	-	0.3952	0.999	0.010
70	Fick	-	0.8106	0.5360	0.996	0.106
	Newton	-	-	0.6497	0.989	0.045
	Henderson and Pabis	-	1.0384	0.6723	0.987	0.042
	Page	1.3359	-	0.5335	0.999	0.010
80	Fick	-	0.8106	0.6901	0.996	0.106
	Newton	-	-	0.8310	0.988	0.043
	Henderson and Pabis	-	1.0195	0.8447	0.987	0.042
	Page	1.3815	-	0.7270	0.999	0.011

Table 3. Effective moisture diffusivity at different temperatures in the convective drying of yacon slabs.

Temperature (°C)	Deff (m^2 s^{-1})
60	$1.22x10^{-10c}$
70	$1.50x10^{-10b}$
80	$1.90x10^{-10a}$

Different letters (a,b,c) within the same column show significant differences between values ($p<0.05$). Data are reported as the mean of three replicates (n=3).

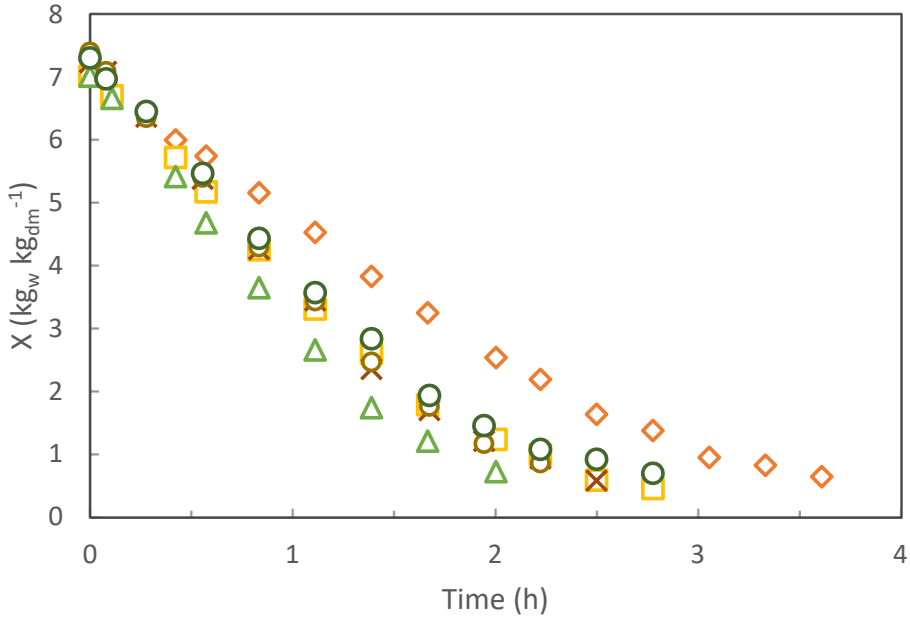

Fig. 3. Convective drying curve of yacon slabs at a temperature of 70 °C and at different air velocities: 0.81 m s^{-1} (◊), 1.2 m s^{-1} (□), 1.46 m s^{-1} (Δ), 1.67 m s^{-1} (X), 1.89 m s^{-1} (O) y 2.06 m s^{-1} (O).

the effect of air velocity becomes negligible. This is because the structural changes in the material create increased internal resistance to moisture transfer (Naderinezhad et al., 2016). Similar findings have been observed in the convective drying of apples (Royen et al., 2020) and the drying of yacon paste at 60 °C (Salinas et al., 2018).

Most dryers have a PID temperature controller that maintains the temperature signal over time. In this way, the error of the signal concerning the reference temperature is minimized. However, this signal can be affected by air velocity. Fig. 4 shows the air temperature signals after heating (TS3) and entering the drying cabin (TS4). As a result, the temperature signals changed with the air velocity, with oscillations of the signals at low air velocities of 0.81 and 1.2 m s^{-1} (Fig. 4 a-b). Similarly, at high air velocities of 1.67 and 1.89 m s^{-1}, the temperature signals were stable, but below the reference temperature (Fig. 4 d-e). By increasing the air velocity to 2.06 m s^{-1}, the signal moved further away from the reference (Fig. 4f).

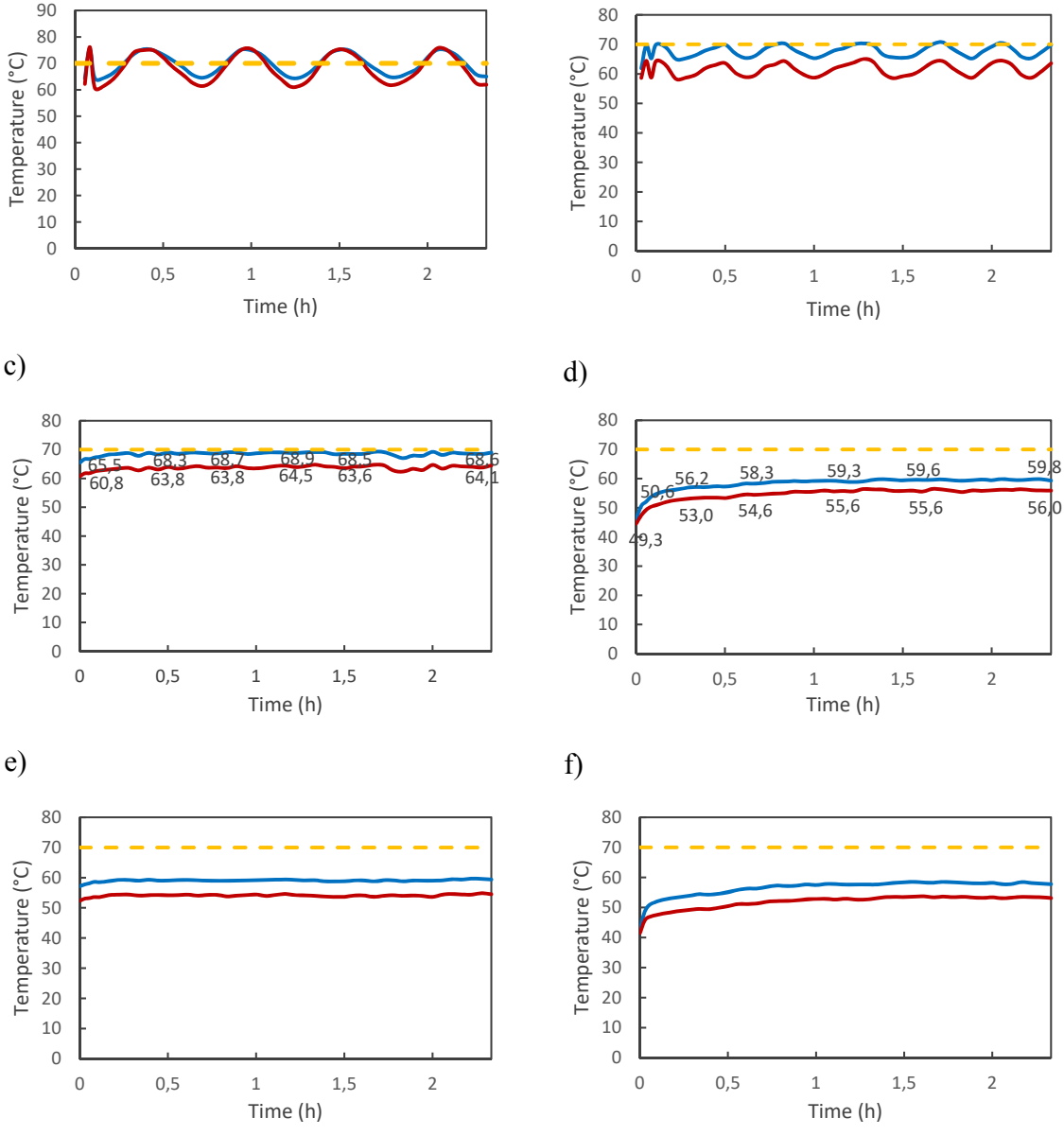

Fig. 4. Temperature signal control in convective drying of yacon slabs at different air velocities: a) 0.81 m s^{-1}, b) 1.2 m s^{-1}, c) 1.46 m s^{-1}, d) 1.67 m s^{-1}, e) 1.89 m s^{-1} y f) 2.06 m s^{-1}. TS3 (——), TS4 (——) y Tr (— —).

In contrast, the temperature signals for TS3 at an air velocity of 1.46 m s^{-1} were closer to the reference and stable (Fig. 4c). Consequently, the error of the temperature signal is smaller compared to the other air velocities. Then, both in the drying kinetics and in the PID temperature control, it was determined that the air velocity for the convective drying of yacon slabs was 1.46 m s^{-1}. Therefore, at air velocities lower than 1.46 m s^{-1}, the temperature signals were oscillatory. Similarly, at air velocities greater than 1.46 m s^{-1}, the temperature signals were below the reference temperature.

Table 4 shows the average temperature, the standard error () and the integral absolute error (IAE) of the temperature signals at different air velocities. As a result, the average drying air temperature for TS3 decreased with increasing air velocity.

When the air velocity was 1.46 m s^{-1} for TS3, the average temperature was 68.4 °C. The absolute error (e_t) was 1.6 concerning the reference temperature of 70 °C, and with was 0.09. However, when the air velocity increased to 2.06 m s^{-1}, the average temperature dropped to 56.25 °C with an e_t of 13.7 and a of 0.31. Consequently, the error rate increases when the air velocity exceeds 1.46 m s^{-1}. Meanwhile, the PID control signals for TS4 showed the same behavior as those for TS3. Temperature signal errors were larger at low and high velocities, but smaller at an air velocity of 1.46 m s^{-1}.

Similarly, Gürel and Ceylan (2014) employed a fluidized bed dryer with a heat pump and PID temperature control to dry mint, parsley, and basil, and obtained nearly identical results with a reference temperature was 40 °C with of ± 0.36 °C. In their investigation of a solar dryer utilizing PID temperature control for potato drying, Herrera-Morales et al. (2022) determined a reference temperature of 36.5 °C±1.24 °C.

Temperature measurements were conducted during the convective drying process of yacon slabs at different air velocities in the TS3 heating zone. At an air velocity of 1.46 m s^{-1}, the average temperature dropped by 2.3% to 68.4 °C. Similarly, at an air velocity of 2.06 m s^{-1}, the average temperature decreased by 19.6% to 56.3 °C compared to the reference temperature. Moving on to the TS4 drying zone, the average temperature experienced an even greater decline at the same air velocity.

In a study conducted by Wutthithanyawat and Srisiriwat (2016) on temperature control in the heating zone, it was found that at an air velocity of 1.20 m s^{-1}, the temperature reached 62.52 °C (control temperature). However, when the air velocity increased to 1.57 m s^{-1}s, the temperature dropped to 57.85 °C, showing a decrease of 6.2% compared to the control. This highlights the importance of considering the impact of air velocity on temperature control.

The yacon dryer comprises a heating zone and a drying zone separated by a distance of 38 cm. Temperature readings for these areas are labeled TS3 and TS4, respectively, with temperature differences between them. It was observed that at an air speed of 0.81 m/s, the temperature dropped 1.6 °C between TS4 and TS3. As the air velocity increased, the temperature dropped between 3.6 and 6.3 °C. The design of the dryer may be considered a limiting factor in this case.

Table 4 shows that TS3 temperature signals displayed a higher integral absolute error (IAE) for both the lowest and highest air velocities. Specifically, the IAE at an air velocity of 1.46 m s^{-1} was 3.21, while it was 30.14 at 2.06 m s^{-1}. In particular, the IAE was lower at the air velocity of 1.46 m s^{-1} compared to other air velocities. Similarly, the temperature signals of TS4 exhibited the same pattern of behavior.

Similar results have been reported in other studies using different drying methods and control systems; to reduce these errors, alternative control systems, such as fuzzy logic control or internal model control, were suggested (Boeri et

Table 4. Average temperature ($\dot{T}$), standard error ($\sigma_{\bar{x}}$) and integral absolute error (IAE) of the temperature signals at different air velocities in convective drying of yacon slabs.

Air velocity, m s^{-1}	$\dot{T} \pm \sigma_{\bar{x}}$		IAE	
	TS3	TS4	TS3	TS4
0.81	69.8 ± 0.62	68.1 ± 0.81	8.14	11.26
1.2	67.7 ± 0.28	61.5 ± 0.33	5.35	19.55
1.46	68.4 ± 0.09	63.6 ± 0.10	3.21	14.31
1.67	58.0 ± 0.27	54.5 ± 0.27	26.16	34.47
1.89	59.0 ± 0.04	54.1 ± 0.05	25.06	36.56
2.06	56.3 ± 0.31	51.6 ± 0.30	30.14	41.17

al., 2013; Wutthithanyawat and Srisiriwat, 2016). Additionally, increasing temperature intervals could be proposed for high air velocities while using PID control (Álvarez de Miguel et al., 2017).

CONCLUSIONS

The drying rate curve indicates that there are two drying phases for yacon: a constant rate phase and a falling rate phase. In terms of modeling drying kinetics, the Page model was identified as the best fit for the ratio of moisture versus time. In addition, the temperature signal during drying was influenced by the air velocity, and the signal exhibited oscillation at low air velocity. At high air velocities, the signal remained stable and significantly deviated from the reference temperature. However, the temperature signal was stable and relatively closer to the reference temperature at an air velocity of 1.46 m s^{-1}. Therefore, air velocity (working range from 0.81 ms^{-1} to 2.06 ms^{-1}) influenced the drying kinetics and PID temperature control during yacon drying.

ACKNOWLEDGEMENTS

We would like to thank Mr. Jairo Purizaca Lachira, Bachelor of Food Science, from the Universidad San Ignacio de Loyola, Lima, Peru, for his assistance in the preliminary laboratory testing of this study.

LITERATURE CITED

AOAC (Association of Official Analytical Chemists). 2005. Official Methods of Analysis. 18th ed. Association of Analytical Chemists, Washington DC, USA.

Álvarez de Miguel, S., J. Mollocana-Lara , C. García-Cena, M. Romero, J. García de María, and J. González-Aguilar. 2017. Identification model and PI and PID controller design for a novel electric air heater. Automatika: Journal for Control, Measurement, Electronics, Computing and Communications 58(1):55-68. doi: 10.1080/00051144.2017.1342958

Amit, S. K., M. M. Uddin, R. Rahman, S. M. Islam, and M. S. Khan. 2017. A review on mechanisms and commercial aspects of food preservation and processing. Agriculture & Food Security 6(1):51. doi: 10.1186/s40066-017-0130-8

Bernstein, A., and C. P. Noreña. 2014. Study of thermodynamic, structural, and quality properties of yacon (*Smallanthus sonchifolius*) during drying. Food and Bioprocess Technology 7(1):148-160. doi:10.1007/s11947-012-1027-y

Boeri, C. N., F. N. Da Silva, and J. Ferreira. 2013. High performance controller for drying processes. Acta Scientiarum. Technology 35(2):279-289. doi: 10.4025/actascitechnol.v35i2.14775

Botelho, F. M., P. C. Corrêa, A. L. Goneli, M. A. Martins, F. E. Magalhães, and S. C. Campos. 2011. Periods of constant and falling-rate for infrared drying of carrot slices. Revista Brasileira de Engenharia Agrícola e Ambiental 15(8):845-852. doi: 10.1590/S1415-43662011000800012

Campos, D., A. Aguilar-Galvez, and R. Pedreschi. 2016. Stability of fructooligosaccharides, sugars and colour of yacon (*Smallanthus sonchifolius*) roots during blanching and drying. International Journal of Food Science & Technology 51(5):1177-1185. doi: 10.1111/ijfs.13074

Castro, A. M., E. Y Mayorga, and F. L. Moreno. 2018. Mathematical modelling of convective drying of fruits: A review. Journal of Food Engineering 223:152-167. doi: 10.1016/j.jfoodeng.2017.12.012

Compaoré, A., A. Putranto, A. O. Dissa, S. Ouoba, R. Rémond, Y. Rogaume, A. Zoulalian, A. Béré, and J. Koulidiati. 2019. Convective drying of onion: modeling of drying kinetics parameters. Journal of Food Science and Technology 56(7):3347-3354. doi: 10.1007/s13197-019-03817-3

Corrêa, J. L., F. J. Lopes, R. E. De Mello Junior, J. R. De Jesus Junqueira, , M. C. De Angelis Pereira, and L. G. Salvio. 2021. Dried yacon with high fructooligosaccharide content. Journal of Food Process Engineering 44(12):e13884. doi: 10.1111/jfpe.13884

Cruz, A. C., R. P. Guiné, and J. C. Gonçalves. 2015. Drying kinetics and product quality for convective drying of apples (cvs. Golden Delicious and Granny Smith). International Journal of Fruit Science 15(1):54-78. doi: 10.1080/15538362.2014.931166

Cuervo, S., A. Benitez, and S. Castellanos. 2018. Drying of yacon (*Smallanthus sonchifolius*) as a potentialfood product for international commercialization. IOP Conference Series: Materials Science and Engineering 437:012005 doi: 10.1088/1757-899X/437/1/012005

Dubey, V., H. Goud, and P. C. Sharma. 2022. Role of PID Control Techniques in Process Control System: A Review. In: Nanda, P., V.K Verma, S. Srivastava, R.K. Gupta, A.P. Mazumdar (eds). Data engineering for smart systems. Lecture Notes in Networks and Systems, Springer, Singapore doi: 10.1007/978-981-16-2641-8_62

Franco, T. S., C. A. Perussello, L. N. Ellendersen, and M. L. Masson. 2017. Effect of process parameters on foam mat drying kinetics of yacon (*Smallanthus sonchifolius*) and thin-layer drying modeling of experimental data. Journal of Food Process Engineering 40(1):e12264. doi: 10.1111/jfpe.12264

Gamboa-Santos, J., A. C. Soria, T. Fornari, M. Villamiel, and A. Montilla. 2013. Optimisation of convective drying of carrots using selected processing and quality indicators. International Journal of Food Science & Technology 48(10):1998-2006. doi: 10.1111/ijfs.12076

Gangta, R., N. S. Thakur, Hamid, S. Gautam, and A. Thakur. 2023. Optimization of pre-drying treatment and drying mode for reducing browning to produce shelf stable fructooligosaccharide rich yacon (Ground Apple) powder. South African Journal of Botany 157:96-105. doi: 10.1016/j.sajb.2023.03.051

Gani, M. M., M. S. Islam, and , M. A. Ullah. 2019. Optimal PID tuning for controlling the temperature of electric furnace by genetic algorithm. SN Applied Sciences 1(8):880. doi: 10.1007/s42452-019-0929-y

Gürel, A. E., and İ. Ceylan. 2014. Thermodynamic analysis of PID temperature controlled heat pump system. Case Studies in Thermal Engineering 2:42-49. doi: 10.1016/j.csite.2013.11.002

Herrera-Morales, J. A., H. Carbajal-Morán, and Á. Almidón-Elescano. 2022. Solar dryer with electronic PID controller for dry potato production. Ecological Engineering & Environmental Technology 23:223-229. doi: 10.12912/27197050/143784

Inyang, U. E., I. O. Oboh, and B. R. Etuk. 2018. Kinetic models for drying techniques-food materials. Advances in Chemical Engineering and Science 8:27-48. doi: 10.4236/aces.2018.82003

Keneni, Y. G., A. K. Hvoslef-Eide, and J. M. Marchetti. 2019. Mathematical modelling of the drying kinetics of *Jatropha curcas* L. seeds. Industrial Crops and Products 132:12-20. doi: 10.1016/j.indcrop.2019.02.012

Khajehei, F., N. Merkt, W. Claupein, and S. Graeff-Hoenninger. 2018. Yacon (*Smallanthus sonchifolius* Poepp. & Endl.) as a novel source of health promoting compounds: antioxidant activity, phytochemicals and sugar content in flesh, peel, and whole tubers of seven cultivars. Molecules 23(2): 278. doi: 10.3390/molecules23020278

Khan, M. I., C. P. Batuwatta-Gamage, M. A. Karim, and Y. Gu. 2022. Fundamental understanding of heat and mass transfer processes for physics-informed machine learning-based drying modelling. Energies 15(24): 9347. doi: 10.3390/en15249347

Khwaja, O., M. H. Siddiqui, and K. Younis. 2020. Underutilized kadam (Neolamarckia cadamba) fruit: Determination of some engineering properties and drying kinetics. Journal of the Saudi Society of Agricultural Sciences 19(6):401-408. doi: 10.1016/j.jssas.2020.06.001

Lisboa, C. G., J. P. Gomes, R. M. Figueirêdo, A. J. Queiroz, A. D. Diógenes, and J. C Melo. 2018. Effective diffusivity in yacon potato cylinders during drying. Revista Brasileira de Engenharia Agrícola e Ambiental 22(8):564-569. dio: 10.1590/1807-1929/agriambi.v22n8p564-569

Mahmood, Q. A., A. T. Nawaf, M. N. Esmael, L. T. Abdulateef, and O. S. Dahham. 2018. PID temperature control of demineralized water tank. IOP Conference Series: Materials Science and Engineering 454:012031. doi: 10.1088/1757-899X/454/1/012031

Marques, B., P. Perré, J. Casalinho, C. C. Tadini, A. Plana-Fattori, and G. Almeida. 2023. Evidence of iso-volume deformation during convective drying of yacón: An extended van Meel model adapted to large volume reduction. Journal of Food Engineering 341:111311. doi: 10.1016/j.jfoodeng.2022.111311

Marques, B. C., A. Plana-Fattori, D. Flick, and C. C. Tadini. 2022a. Convective drying of yacón (*Smallanthus sonchifolius*) slices: A simple physical model including shrinkage. LWT 159:113151. doi: 10.1016/j.lwt.2022.113151

Marques, B. C., A. Plana-Fattori, C. C. Tadini, and D. Flick. 2022b. Modeling convective drying of food products: the case study of yacon (*Smallanthus sonchifolius*). 12th International Conference on Simulation and Modelling in the Food and Bio-Industry (FOODSIM'2022)

Mejía-Águila, R. A., A. Aguilar-Galvez, R. Chirinos, R. Pedreschi, and D. Campos. 2021. Vacuum impregnation of apple slices with Yacon (*Smallanthus sonchifolius* Poepp. & Endl) fructooligosaccharides to enhance the functional properties of the fruit snack. International Journal of Food Science & Technology 56(1):392-401. doi: 10.1111/ijfs.14654

Naderinezhad, S., N. Etesami, A. Poormalek Najafabady, and M. Ghasemi Falavarjani. 2016. Mathematical modeling of drying of potato slices in a forced convective dryer based on important parameters. Food Science & Nutrition 4(1):110-118. doi: 10.1002/fsn3.258

Oliveira, G. O., C. P. Braga, and A. A. Fernandes. 2013. Improvement of biochemical parameters in type 1 diabetic rats after the roots aqueous extract of yacon [*Smallanthus sonchifolius* (Poepp.& Endl.)] treatment. Food and Chemical Toxicology 59:256-260. doi: 10.1016/j.fct.2013.05.050

Oliveira, L. F., J. L. Corrêa, P. G. Silveira, M. B. Vilela, and J. R. Junqueira. 2021. Drying of 'yacon' pretreated by pulsed vacuum osmotic dehydration. Revista Brasileira de Engenharia Agrícola e Ambiental 25. doi: 10.1590/1807-1929/agriambi.v25n8p560-565

Razola-Díaz, M. D., V. Verardo, A. M. Gómez-Caravaca, B. García-Villanova, and E. J. Guerra-Hernández. 2023. Mathematical modelling of convective drying of orange by-product and its influence on phenolic compounds and ascorbic acid content, and its antioxidant activity. Foods 12(3)500. doi: 10.3390/foods12030500

Royen, M. J., A. W. Noori, and J. Haydary. 2020. Experimental study and mathematical modeling of convective thin-layer drying of apple slices. Processes 8(12):1562. doi: 10.3390/pr8121562.

Sahoo, M., S. Titikshya, P. Aradwad, V. Kumar, and S. N. Naik. 2022. Study of the drying behaviour and color kinetics of convective drying of yam (*Dioscorea hispida*) slices. Industrial Crops and Products 176:114258. doi: 10.1016/j.indcrop.2021.114258

Salinas, J. G., J. A. Alvarado, B. Bergenståhl, and E. Tornberg. 2018. The influence of convection drying on the physicochemical properties of yacón (*Smallanthus sonchifolius*). Heat and Mass Transfer 54(10):2951-2961. doi: 10.1007/s00231-018-2334-2

Shi, Q., Y. Zheng, and Y. Zhao. 2013. Mathematical modeling on thin-layer heat pump drying of yacon (*Smallanthus sonchifolius*) slices. Energy Conversion and Management 71:208-216. doi: 10.1016/j.enconman.2013.03.032

Simal, S., A. Femenia, M. C.Garau, and C. Rosselló. 2005. Use of exponential, Page's and diffusional models to simulate the drying kinetics of kiwi fruit. Journal of Food Engineering 66(3):323-328. doi: 10.1016/j.jfoodeng.2004.03.025

Sungthong, A., and W. Assawinchaichote. 2016. Particle swam optimization based optimal PID parameters for air heater temperature control system. Procedia Computer Science 86:108-111. doi: 10.1016/j.procs.2016.05.027

Wu, Z., D. Li, and Y. Xue. 2019. A New PID controller design with constraints on relative delay margin for first-order plus dead-time systems. Processes 7(10):713. doi: 10.3390/pr7100713

Wutthithanyawat, C., and N. Srisiriwat. 2016. Temperature control of heating zone for drying process: effect of air velocity change. MATEC Web of Conferences 65:03002. doi: 10.1051/matecconf/20166503002

Zheng, Z., S. Wang, C. Zhang, M. Wu, D. Cui, X. Fu, L. Gao, A. Li, Q. Wei, and Z. Liu. 2023. Hot Air Impingement Drying Enhanced Drying Characteristics and Quality Attributes of Ophiopogonis Radix. Foods 12(7):1441. doi: 10.3390/foods12071441